Journal of Sound and Vibration (2002) **253**(2), 373–388
doi:10.1006/jsvi.2001.4047 available online at http://www.idealibrary.com on IDEAL®

RITZ VECTOR APPROACH FOR STATIC AND DYNAMIC ANALYSIS OF PLATES WITH EDGE BEAMS

J. Yang and A. Gupta

Department of Civil Engineering, North Carolina State University, Raleigh, NC 27695-7908, *U.S.A.*,
E-mail: *agupta1@eos.ncsu.edu*

(*Received* 25 *April* 2001, *and in final form* 14 *September* 2001)

A Ritz vector approach is used to develop new formulations for evaluating the static and the dynamic characteristics of rectangular plates with edge beams. Unlike previous studies in which stiffness coefficients with specified distributions along the plate edges are used to represent the effect of edge restraints, the effect of elastic edge restraints is accounted for by including appropriate integrals for edge beams in the expressions for total kinetic and potential energies in a Rayleigh–Ritz approach. The effect of various types of boundary conditions at the beam ends is accounted for by considering the corresponding Ritz vectors. The contribution of beam mass to the total kinetic energy is also considered in the proposed approach. This effect has often been neglected in the previous studies but can be significant in some applications. The results obtained from the application of the proposed approach to a variety of examples are compared with the corresponding results obtained from the finite element analysis.

1. INTRODUCTION

Transverse vibration of plates with edge beams has been widely investigated in a variety of applications that include aerospace, civil, naval, and power plant structural systems. Leissa *et al.* [1] presented some of the early developments in this subject and summarized the problems associated with it. Takabatake and Nagareda [2] categorized the research on elastically restrained plates into two types: (1) formulation of the governing equations, and (2) analytical methods for the solution of these equations in plates with different types of boundary conditions. Takabatake and co-workers [3–6] presented the governing equations for various types of rectangular and circular plates under Kirchoff–Love hypotheses whereas Laura and Grossi [7] studied the transverse vibration of rectangular plates with elastic translational and rotational edge restraints. Warburton and Edney [8] used Rayleigh–Ritz approach in which a pair of Ritz vectors corresponding to two different idealized boundary conditions is selected for representing an intermediate boundary condition thereby avoiding the problem associated with the selection of Ritz vectors in plates with elastic edge restraints. The two Ritz vectors are then used to develop an eigenvalue problem for evaluating the fundamental frequency. Gorman [9] used the method of superposition to provide useful generalized solutions for plates with arbitrarily distributed translational and rotational restraints along the edges. The translational and rotational restraints in these studies were represented in terms of stiffness coefficients having specified distributions along the plate edge. Although these formulations provide accurate solutions, they could not be applied directly to a majority of practical situations wherein the distribution of elastic restraints along the plate edges cannot be determined. For example, the variation of translational and rotational restraints provided by the presence of additional structural members such as beams along the plate edges is dependent upon not only the beam cross-section but also the boundary conditions at the beam ends. The distribution of these stiffness coefficients cannot be easily determined *a priori*. Takabatake and Nagareda [2] developed a simplified analytical method under the assumption of Kirchoff–Love hypotheses using Galerkin method to overcome this limitation. New formulations are provided for initial selection of the stiffness coefficients. These initial values and the shape functions are then improved iteratively by the convergence of maximum deflection and natural frequency. However, the translational and the rotational stiffness coefficients calculated from the new formulations are then assumed to be uniformly distributed over the entire length of plate edges. Results obtained from the application of this method to different examples are validated by comparison with the results evaluated from the corresponding finite element analyses. In this paper, we present an alternate method for static and dynamic analyses of elastic plates with edge beams. It is based on the useful insights provided by Warburton and Edney [8] as well as Takabatake and Nagareda [2], and employs static beam functions in Rayleigh–Ritz method to account for the actual bending and torsional stiffness of edge beams. The proposed approach is not based on any assumption regarding the distribution of translational and rotational stiffness imparted by the edge beams.

2. GOVERNING EQUATIONS FOR A PLATE WITH EDGE BEAMS

Consider an isotropic rectangular uniform plate with edge beams, as shown in Figure 1. Assuming that the Kirchoff–Love hypotheses is valid, the equation of motion for the transverse plate vibration can be written as

$$m_0\frac{\partial^2 w}{\partial t^2} + c\frac{\partial w}{\partial t} + D_0\left(\frac{\partial^4 w}{\partial x^4} + 2\frac{\partial^4 w}{\partial x^2 \partial y^2} + \frac{\partial^4 w}{\partial y^4}\right) = p, \tag{1}$$

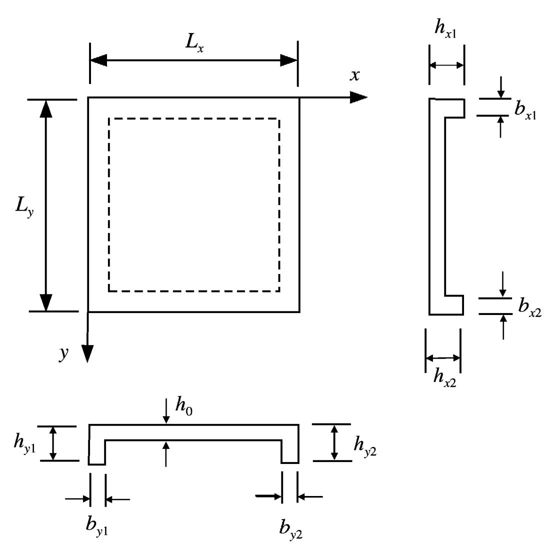

Figure 1. Rectangular plate with edge beams.

in which m_0 is the mass per unit area; w is the transverse displacement of the plate as a function of co-ordinates x, y and time t; c is the damping coefficient; D_0 is the flexural rigidity of the plate; and p is the external load. Expressions for the boundary conditions in a plate supported on edge beams are expressed by Vinson [10] as follows:

(1) *Boundary conditions* at $x = 0$ *and* L_x:

$$-D_0\left[\frac{\partial^3 w}{\partial x^3} + (2-v)\frac{\partial^3 w}{\partial x \partial y^2}\right] = (EI_{x1})^b\,\frac{\partial^4 w}{\partial y^4} \quad \text{at } x = 0, \tag{2}$$

$$-D_0\left[\frac{\partial^2 w}{\partial x^2} + v\,\frac{\partial^2 w}{\partial y^2}\right] = (GJ_{x1})^b\,\frac{\partial^3 w}{\partial x \partial y^2} \quad \text{at } x = 0, \tag{3}$$

$$-D_0\left[\frac{\partial^3 w}{\partial x^3} + (2-v)\,\frac{\partial^3 w}{\partial x \partial y^2}\right] = (EI_{x2})^b\,\frac{\partial^4 w}{\partial y^4} \quad \text{at } x = L_x, \tag{4}$$

$$-D_0\left[\frac{\partial^2 w}{\partial x^2} + v\,\frac{\partial^2 w}{\partial y^2}\right] = (GJ_{x2})^b\frac{\partial^3 w}{\partial x \partial y^2} \quad \text{at } x = L_x. \tag{5}$$

(2) *Boundary conditions at* $y = 0$ *and* L_y:

$$-D_0\left[\frac{\partial^3 w}{\partial y^3} + (2-v)\,\frac{\partial^3 w}{\partial x^2 \partial y}\right] = (EI_{y1})^b\,\frac{\partial^4 w}{\partial x^4} \quad \text{at } y = 0, \tag{6}$$

$$-D_0\left[\frac{\partial^2 w}{\partial y^2} + v\,\frac{\partial^2 w}{\partial x^2}\right] = (GJ_{y1})^b\,\frac{\partial^3 w}{\partial x^2 \partial y} \quad \text{at } y = 0, \tag{7}$$

$$-D_0\left[\frac{\partial^3 w}{\partial x^3} + (2-v)\,\frac{\partial^3 w}{\partial x \partial y^2}\right] = (EI_{y2})^b\frac{\partial^4 w}{\partial y^4} \quad \text{at } y = L_y, \tag{8}$$

$$-D_0\left[\frac{\partial^2 w}{\partial y^2} + v\,\frac{\partial^2 w}{\partial x^2}\right] = (GJ_{y2})^b\,\frac{\partial^3 w}{\partial x^2 \partial y} \quad \text{at } y = L_y, \tag{9}$$

and $w = 0$ at the corners. The terms $(EI_{x1})^b, (EI_{x2})^b, \ldots$ and $(GJ_{x1})^b, (GJ_{x2})^b, \ldots$ in the above equations represent the bending and the torsional stiffness of the edge beams. The superscript b is used to denote the quantities for edge beams whereas the subscripts $x1, x2$ and $y1, y2$ are used to represent the beams that are parallel to x- and y-axis respectively.

Takabatake and Nagareda [2] proposed new formulations to evaluate the stiffness coefficients for the translational and the rotational stiffness of supporting edge beams in which the deflection of an edge beam is represented by a sinusoidal function to evaluate the initial values of the stiffness coefficients that are then improved iteratively. Further, the effect of slab on the beam stiffness coefficients is accounted for by using two additional factors, ϕ_B and ϕ_J, for the terms corresponding to the bending and the torsion respectively. These factors have different values for the beams that are simply supported and for the beams that are clamped at their ends. The factors are determined based on engineering and professional experience. For simplicity, Takabatake and Nagareda [2] assume the stiffness coefficients calculated by the new formulations to be uniformly distributed over the entire length of plate edge. The assumptions made in this approach may be avoided by combining it with the method proposed by Warburton and Edney [8]. Instead of considering the stiffness coefficients to be uniformly distributed along the length, the bending and the torsion characteristics of the beam can be considered by incorporating appropriate integrals in the expressions for total kinetic and potential energies. An eigenvalue problem for transverse plate vibration may then be developed using these expressions in a Ritz-vector-based Lagrangian approach.

3. FREE VIBRATION ANALYSIS

Let us express the transverse displacement w of a plate at any instant t as a summation of Ritz vectors

$$w(x,y,t)=\sum_{r=1}^{n} q_r(t)\phi_r(x,y), \tag{10}$$

where $q_r(t)$ represent the generalized co-ordinates as a function of time t, and $\phi_r(x,y)$ the Ritz vectors as functions of co-ordinates x and y. For rectangular plates, $\phi_r(x,y)$ can be further simplified as

$$\phi_r(x,y)=\phi_{xr}(x)\phi_{yr}(y). \tag{11}$$

Each of the two Ritz vectors $\phi_{xr}(x)$ and $\phi_{yr}(y)$ are normalized to unity. Thus, the motion at a given location is linearly transformed into an n-degree-of-freedom (d.o.f) system using the above equations. Eigenvalue problem of this generalized n-.d.o.f. system can be written as

$$\mathbf{Kq}=\omega^2\mathbf{Mq}, \tag{12}$$

where $\mathbf{K}$ and $\mathbf{M}$ are the equivalent stiffness and mass matrices, respectively, and $\mathbf{q}$ is the vector of normal co-ordinates. Solution of the eigenvalue problem gives the plate frequencies and the corresponding eigenvectors. The jth mode shape can be expressed using the elements of the jth eigenvector $\mathbf{q}_j$ as

$$\psi_j(x,y)=\sum_{i=1}^{n} q_{ji}\phi_{xi}(x)\phi_{yi}(y). \tag{13}$$

4. EQUIVALENT MASS AND STIFFNESS MATRICES

The kinetic energy, T, of a plate with edge beams is given by

$$T=T_p+T_{xb}+T_{yb}, \tag{14}$$

in which T_p, T_{xb}, and T_{yb} are the kinetic energy contributions of the plate, the edge beams parallel to the x-axis, and the edge beams parallel to the y-axis respectively. The kinetic energy, T_p, of a rectangular plate having uniform thickness h_0, and mass density ρ is given by

$$T_p=\frac{\rho h_0}{2}\int_0^{L_x}\int_0^{L_y}\left(\frac{\partial w}{\partial t}\right)^2 \mathrm{d}x\,\mathrm{d}y, \tag{15}$$

where L_x is the plate dimension along the x-axis and L_y that along the y-axis. The kinetic energy contributions of the edge beams, T_{xb} and T_{yb}, can be written as

$$T_{xb}=\frac{\mu_{x1}}{2}\int_0^{L_x}\left(\frac{\partial w}{\partial t}\right)^2(x,y=y_1)\,\mathrm{d}x+\frac{\mu_{x2}}{2}\int_0^{L_x}\left(\frac{\partial w}{\partial t}\right)^2(x,y=y_2)\,\mathrm{d}x, \tag{16}$$

$$T_{yb}=\frac{\mu_{y1}}{2}\int_0^{L_y}\left(\frac{\partial w}{\partial t}\right)^2(x=x_1,y)\,\mathrm{d}y+\frac{\mu_{y2}}{2}\int_0^{L_y}\left(\frac{\partial w}{\partial t}\right)^2(x=x_2,y)\,\mathrm{d}y, \tag{17}$$

in which μ_{xj} and μ_{yi} represent the mass per unit length of jth edge beam parallel to the x-axis located at a distance y_j from the origin, and ith edge beam parallel to the y-axis located at a distance of x_i from the origin respectively.

The potential energy, U, of a plate with edge beams is given by

$$U = U_p + U_{xb} + U_{yb}, \tag{18}$$

where U_p, U_{xb}, and U_{yb} are the potential energy contributions of the plate, the edge beams parallel to the x-axis and the edge beams parallel to the y-axis respectively. Further,

$$U_p = \frac{Eh_0^3}{24(1-v^2)} \int_0^{L_x} \int_0^{L_y} \left[\left(\frac{\partial^2 w}{\partial x^2} \right)^2 + 2v \frac{\partial^2 w}{\partial x^2} \frac{\partial^2 w}{\partial y^2} + 2(1-v) \left(\frac{\partial^2 w}{\partial x \partial y} \right)^2 + \left(\frac{\partial^2 w}{\partial y^2} \right)^2 \right] \mathrm{d}x\, \mathrm{d}y, \tag{19}$$

in which E and v are Young's modulus of elasticity and the Poisson ratio for plate material. U_{xb} and U_{yb} are given by

$$U_{xb} = U_{xb1} + U_{xb2}, \tag{20}$$

$$U_{xb1,2} = \frac{EI_{x1,2}}{2} \int_0^{L_x} \left(\sum_r q_r \frac{\partial^2 \phi_{xr}}{\partial x^2} \phi_{yr}(y = y_{1,2}) \right)^2 \mathrm{d}x + \frac{GJ_{x1,2}}{2} \int_0^{L_x} \left(\sum_r q_r \frac{\partial \phi_{xr}}{\partial x} \frac{\partial \phi_{yr}}{\partial y}(y = y_{1,2}) \right)^2 \mathrm{d}x, \tag{21}$$

$$U_{yb} = U_{yb1} + U_{yb2}, \tag{22}$$

$$U_{yb1,2} = \frac{EI_{y1,2}}{2} \int_0^{L_y} \left(\sum_r q_r \phi_{xr}(x = x_{1,2}) \frac{\partial^2 \phi_{yr}}{\partial y^2} \right)^2 \mathrm{d}y + \frac{GJ_{y1,2}}{2} \int_0^{L_y} \left(\sum_r q_r \frac{\partial \phi_{xr}}{\partial x}(x = x_{1,2}) \frac{\partial \phi_{yr}}{\partial y} \right)^2 \mathrm{d}y, \tag{23}$$

where $I_{x1,2}$ represents the moment of inertia for the edge beams parallel to the x-axis and $I_{y1,2}$ that for the edge beams parallel to the y-axis. Similarly, $J_{x1,2}$ and $J_{y1,2}$ represent the corresponding torsion constants. G is the shear modulus for the beam material. According to Lagrangian approach, the equation of motion for undamped free vibration can be expressed as

$$\frac{\partial}{\partial t}\left(\frac{\partial T}{\partial \dot{q}_r} \right) + \frac{\partial U}{\partial q_r} = 0, \tag{24}$$

in which q_r is used to represent the generalized co-ordinate $q_r(t)$ and $\dot{q}_r$ is its time derivative. Therefore, the elements of equivalent mass matrix can be evaluated using n equations obtained by differentiating T with respect to the $\dot{q}_r$'s:

$$\frac{\partial}{\partial t}\left(\frac{\partial T}{\partial \dot{q}_r} \right) = \sum_{s=1}^{n} m_{rs} \ddot{q}_s. \tag{25}$$

The elements, m_{rs}, of the equivalent mass matrix, $\mathbf{M}$, for the plate with edge beams are given by

$$m_{rs} = m_{rs}^p + m_{rs}^{xb} + m_{rs}^{yb}, \tag{26}$$

$$m_{rs}^p = \rho h_0 \int_0^{L_x} \phi_{xr} \phi_{xs}\, \mathrm{d}x \int_0^{L_y} \phi_{yr} \phi_{ys}\, \mathrm{d}y, \tag{27}$$

$$m_{rs}^{xb} = \mu_{x1}\phi_{yr}(y=y_1)\phi_{ys}(y=y_1)\int_0^{L_x}\phi_{xr}\phi_{xs}\,\mathrm{d}x + \mu_{x2}\phi_{yr}(y=y_2)\phi_{ys}(y=y_2)\int_0^{L_x}\phi_{xr}\phi_{xs}\,\mathrm{d}x, \tag{28}$$

$$m_{rs}^{yb} = \mu_{y1}\phi_{xr}(x=x_1)\phi_{xs}(x=x_1)\int_0^{L_y}\phi_{yr}\phi_{ys}\,\mathrm{d}y + \mu_{y2}\phi_{xr}(x=x_2)\phi_{xs}(x=x_2)\int_0^{L_y}\phi_{yr}\phi_{ys}\,\mathrm{d}y,$$

$$r=1,\ldots,n, \quad s=1,\ldots n. \tag{29}$$

Likewise, differentiating U with respect to the q_r's yields n equations of the form

$$\frac{\partial U}{\partial q_r} = \sum_{s=1}^{n} k_{rs}q_s. \tag{30}$$

The elements, k_{rs}, of the equivalent stiffness matrix, $\mathbf{K}$, are given by

$$k_{rs} = k_{rs}^{p} + k_{rs}^{xbI} + k_{rs}^{ybI} + k_{rs}^{xbJ} + k_{rs}^{ybJ}, \tag{31}$$

$$k_{rs}^{p} = \frac{Eh_0^3}{12(1-v^2)}(k_{rs}^{p1} + k_{rs}^{p2} + k_{rs}^{p3} + k_{rs}^{p4}), \tag{32}$$

$$k_{rs}^{p1} = \int_0^{L_x}\frac{\partial^2\phi_{xr}}{\partial x^2}\frac{\partial^2\phi_{xs}}{\partial x^2}\,\mathrm{d}x\int_0^{L_y}\phi_{yr}\phi_{ys}\,\mathrm{d}y, \tag{33}$$

$$k_{rs}^{p2} = v\int_0^{L_x}\frac{\partial^2\phi_{xr}}{\partial x^2}\phi_{xs}\,\mathrm{d}x\int_0^{L_y}\phi_{yr}\frac{\partial^2\phi_{ys}}{\partial y^2}\,\mathrm{d}y + v\int_0^{L_x}\phi_{xr}\frac{\partial^2\phi_{xs}}{\partial x^2}\,\mathrm{d}x\int_0^{L_y}\frac{\partial^2\phi_{yr}}{\partial y^2}\phi_{ys}\,\mathrm{d}y, \tag{34}$$

$$k_{rs}^{p3} = 2(1-v)\int_0^{L_x}\frac{\partial\phi_{xr}}{\partial x}\frac{\partial\phi_{xs}}{\partial x}\,\mathrm{d}x\int_0^{L_y}\frac{\partial\phi_{yr}}{\partial y}\frac{\partial\phi_{ys}}{\partial y}\,\mathrm{d}y, \tag{35}$$

$$k_{rs}^{p4} = \int_0^{L_x}\phi_{xr}\phi_{xs}\,\mathrm{d}x\int_0^{L_y}\frac{\partial^2\phi_{yr}}{\partial y^2}\frac{\partial^2\phi_{ys}}{\partial y^2}\,\mathrm{d}y, \tag{36}$$

$$k_{rs}^{xbI} = EI_{x1}\phi_{yr}(y=y_1)\phi_{ys}(y=y_1)\int_0^{L_x}\frac{\partial^2\phi_{xr}}{\partial x^2}\frac{\partial^2\phi_{xs}}{\partial x^2}\,\mathrm{d}x + EI_{x2}\phi_{yr}(y=y_2)\phi_{ys}(y=y_2)\int_0^{L_x}\frac{\partial^2\phi_{xr}}{\partial x^2}\frac{\partial^2\phi_{xs}}{\partial x^2}\,\mathrm{d}x, \tag{37}$$

$$k_{rs}^{ybI} = EI_{y1}\phi_{xr}(x=x_1)\phi_{xs}(x=x_1)\int_0^{L_y}\frac{\partial^2\phi_{yr}}{\partial y^2}\frac{\partial^2\phi_{ys}}{\partial y^2}\,\mathrm{d}y + EI_{y2}\phi_{xr}(x=x_2)\phi_{xs}(x=x_2)\int_0^{L_y}\frac{\partial^2\phi_{yr}}{\partial y^2}\frac{\partial^2\phi_{ys}}{\partial y^2}\,\mathrm{d}y, \tag{38}$$

$$k_{rs}^{xbJ} = GJ_{x1}\int_0^{L_x}\frac{\partial\phi_{xr}}{\partial x}\frac{\partial\phi_{xs}}{\partial x}\frac{\partial\phi_{yr}}{\partial y}(y=y_1)\frac{\partial\phi_{ys}}{\partial y}(y=y_1)\,\mathrm{d}x + GJ_{x2}\int_0^{L_x}\frac{\partial\phi_{xr}}{\partial x}\frac{\partial\phi_{xs}}{\partial x}\frac{\partial\phi_{yr}}{\partial y}(y=y_2)\frac{\partial\phi_{ys}}{\partial y}(y=y_2)\,\mathrm{d}x, \tag{39}$$

$$k_{rs}^{ybJ} = GJ_{y1} \int_0^{L_y} \frac{\partial \phi_{xr}}{\partial x}(x = x_1) \frac{\partial \phi_{xs}}{\partial x}(x = x_1) \frac{\partial \phi_{yr}}{\partial y} \frac{\partial \phi_{ys}}{\partial y}\, \mathrm{d}y$$

$$+ GJ_{y2} \int_0^{L_y} \frac{\partial \phi_{xr}}{\partial x}(x = x_2) \frac{\partial \phi_{xs}}{\partial x}(x = x_2) \frac{\partial \phi_{yr}}{\partial y} \frac{\partial \phi_{ys}}{\partial y}\, \mathrm{d}y,$$

$$r = 1, \ldots, n, \quad s = 1, \ldots, n. \tag{40}$$

The above formulations are written for a generalized case wherein n Ritz vectors are used in equation (10) to evaluate the response quantity of interest. Later, we illustrate that only a few Ritz vectors are needed in the application of this approach to real-life problems. Once the Ritz vectors needed in the solution of a particular problem are identified, the various terms in the above equations can be calculated either numerically or closed form. It should be noted that the various stiffness terms corresponding to edge beams give equivalent distributions of the bending and the torsion stiffness at the plate edges. However, these distributions cannot be used directly in the method presented by other researchers such as that by Gorman [9]. Another difference of the proposed formulations from the existing formulations is evident in the expressions for the elements of the equivalent mass matrix. The mass participation of edge beams can be significant and unlike many previous studies, its effect is included in the proposed approach. Further discussion on the number and the nature of Ritz vectors needed in an analysis is presented in the next section.

5. SELECTION OF RITZ VECTORS

Accuracy of the calculated response quantities in the Rayleigh–Ritz method depends on the selection of Ritz vectors which in turn depends upon the boundary conditions at the plate edges and beam ends. Several mathematical functions have been proposed as Ritz vectors by various researchers for idealized boundary conditions [11–15]. In this paper, we use simple and easy-to-use mathematical functions given by Blevins [11].

For plates that are restrained elastically by the edge beams, more than one simple Ritz vector may be needed. As stated earlier, Warburton and Edney [8] proposed such an approach in which two Ritz vectors corresponding to two different idealized boundary conditions are considered for representing an intermediate boundary condition. Several (ideally infinite) vectors can be used in this procedure. However, the computational complexity increases as additional Ritz vectors are included in the analysis. Table 1 gives some examples of typical mathematical functions that can be used as Ritz vectors for a few idealized boundary conditions.

For rectangular plates, selection of Ritz vectors requires evaluation of two boundary conditions at each edge, one for the out-of-plane translation and the other for the rotation about the plate edge. Let us consider a plate shown in Figure 2 to illustrate the selection of Ritz vectors. The plate has beams on all four edges which are restrained against out-of-plane translation as well as rotation at their ends (plate's corners). The beam at any particular edge can deform in bending thus allowing an out-of-plane translation at the plate edge. Similarly, the beam may also undergo a torsional deformation allowing a rotation about the plate edge. The degree of translation and rotation at a particular plate edge is governed by the beam's bending and the torsional stiffness, as shown in equations (37–40). For a beam with relatively large bending stiffness and low torsional stiffness, the out-of-plane translation is negligible and the boundary condition converges to that of a

TABLE 1

Ritz vectors for idealized boundary conditions

Description	Ritz vector
Clamped–clamped ϕ_{cc}	$\cosh\frac{\lambda x}{L}-\cos\frac{\lambda x}{L}-\sigma\left(\sinh\frac{\lambda x}{L}-\sin\frac{\lambda x}{L}\right)$ $\lambda=4{\cdot}73004074,\ \sigma=0{\cdot}982502215$
Pinned–pinned ϕ_{pp}	$\sin\frac{\pi x}{L}$
Clamped–pinned ϕ_{cp}	$\cosh\frac{\lambda x}{L}-\cos\frac{\lambda x}{L}-\sigma\left(\sinh\frac{\lambda x}{L}-\sin\frac{\lambda x}{L}\right)$ $\lambda=3{\cdot}92660231,\ \sigma=1{\cdot}000777304$
Sliding–pinned ϕ_{sp}	$\cos\frac{\pi x}{2L}$
Clamped–sliding ϕ_{cs}	$\cosh\frac{\lambda x}{L}-\cos\frac{\lambda x}{L}-\sigma\left(\sinh\frac{\lambda x}{L}-\sin\frac{\lambda x}{L}\right)$ $\lambda=2{\cdot}36502037,\ \sigma=0{\cdot}982502207$
Free–free ϕ_{ff}	1

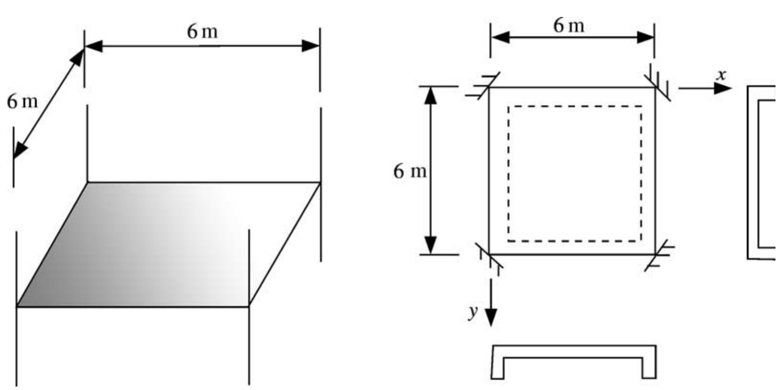

Figure 2. Elastic plate with edge beams, clamped at corners.

pinned support. Similarly, in a beam with relatively high values of both the bending and the torsional stiffness, not only is the out-of-plane translation negligible but also the rotation about the plate edge. For such a beam, the boundary condition at the plate's edge converges to that of a clamped support. In addition to the pinned and clamped boundary conditions, an additional limiting condition corresponds to that of a free edge when the values for both the bending as well as the torsional beam stiffness are relatively small. Consequently, three Ritz vectors corresponding to clamped, pinned, and free boundary conditions at a particular edge are needed to accurately account for the bending and the torsional beam stiffness in a generalized solution. However, an additional (fourth) Ritz vector is needed to account for the restraints at the beam ends (plate's corners). For the plate shown in Figure 2, all the four corners are considered to be clamped. Therefore, an additional Ritz vector for clamped–clamped condition is needed in the directions parallel to the x as well as the y axes. Therefore, equation (10) can be written as

$$w(x,y,t) = q_1(t)\phi_{cc}\phi_{cc} + q_2(t)\phi_{pp}\phi_{pp} + q_3(t)\phi_{cc}\phi_{ff} + q_4(t)\phi_{ff}\phi_{cc}. \tag{41}$$

Next, let us consider that the particular plate shown in Figure 2 is 0·12 m thick and has span lengths, L_x and L_y, equal to 6 m. The properties for the plate material are: $E = 2{\cdot}06 \times 10^4$ Mpa, $v = 0{\cdot}17$ and $\rho = 2400\,\mathrm{kg/m^3}$. Further, all the four beams supporting the plate are identical with moment of inertia equal to $0{\cdot}00933\,\mathrm{m}^4$ and the torsion constant equal to $0{\cdot}0048\,\mathrm{m}^4$. The mass per unit length for each beam is 518·4 kg/m.

The fundamental frequency for the transverse vibration of this plate calculated by using equation (41) in the proposed approach is 14·0 Hz which is close to 13·9 Hz calculated from a detailed finite element analysis. A comparison of the plate's fundamental mode shape evaluated from the two methods is shown in Figures 3 and 4.

To illustrate the effect of boundary conditions at the beam ends, let us consider a modification of the above example so that the plate can undergo unrestrained rotation at

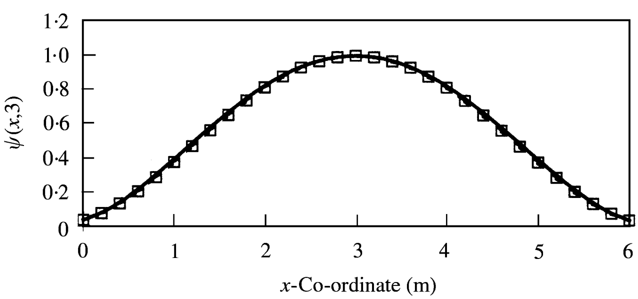

Figure 3. Fundamental mode shape at $y = 3$ m, plate with clamped corners: —, finite element; --□--, Ritz vector.

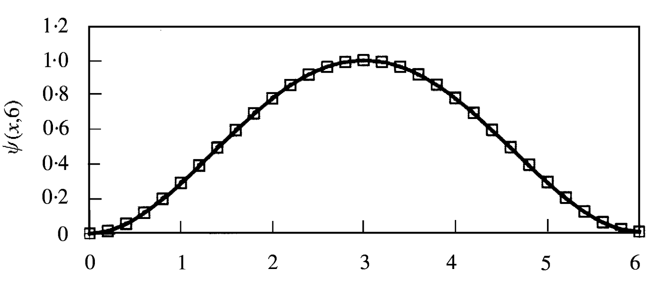

Figure 4. Fundamental mode shape at $y = 6$ m, plate with clamped corners: —, finite element; --□--, Ritz vector.

all the four corners, i.e., the plate is considered to be simply supported at the corners. The fundamental frequency of the modified plate–beam system as evaluated from a finite element analysis is equal to 10·8 Hz. To solve this problem using the proposed approach, equation (41) is re-written as

$$w(x, y, t) = q_1(t)\phi_{cc}\phi_{cc} + q_2(t)\phi_{pp}\phi_{pp} + q_3(t)\phi_{pp}\phi_{ff} + q_4(t)\phi_{ff}\phi_{pp}, \quad (42)$$

in which the Ritz vector for clamped–clamped boundary conditions at beam ends is replaced by that for pinned–pinned boundary conditions. The fundamental frequency calculated by using the above equation equals 10·9 Hz and is close to 10·8 Hz calculated from the finite element analysis. Similarly, the mode shapes from the two sets of analyses are also close, as shown in Figures 5 and 6.

In the above example, contribution of the beam's kinetic energy to the total kinetic energy of the system is considered in both the Ritz vector approach as well as the finite element analysis. This effect has often been neglected in the previous studies. To illustrate the significance of this effect, a series of solutions were evaluated for the example described above by varying the mass per unit length of the edge beams. For a plate with simply supported corners, Figure 7 shows a comparison of the fundamental frequencies evaluated by considering the effect of beam mass with those evaluated by neglecting it. As shown in the figure, this effect can be significant and should be considered.

A fewer number of Ritz vectors are needed in the proposed approach if the boundary conditions at a particular plate edge can be estimated to be close to idealized conditions. For the plate shown in Figure 8, the out-of-plane translation is restrained at all four edges

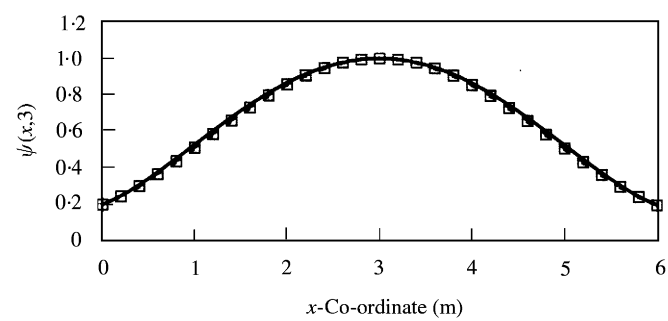

Figure 5. Fundamental mode shape at $y = 3$ m, plate with simply supported corners: —, finite element; - -□- -, Ritz vector.

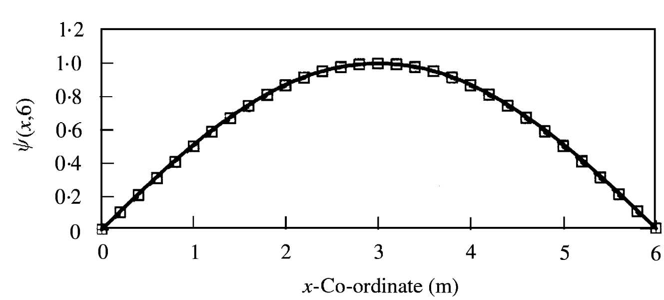

Figure 6. Fundamental mode shape at $y = 6$ m, plate with simply supported corners: —, finite element; - -□- -, Ritz vector.

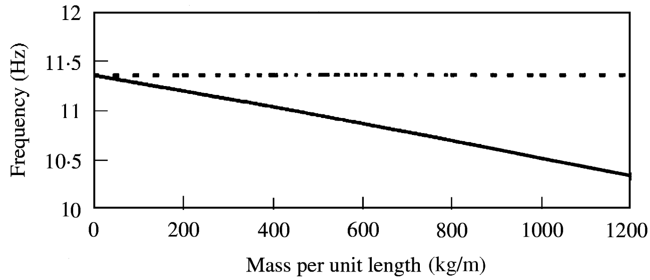

Figure 7. Variation of fundamental frequency with edge beam mass, plate with simply supported corners: —, beam mass included; ----, beam mass neglected.

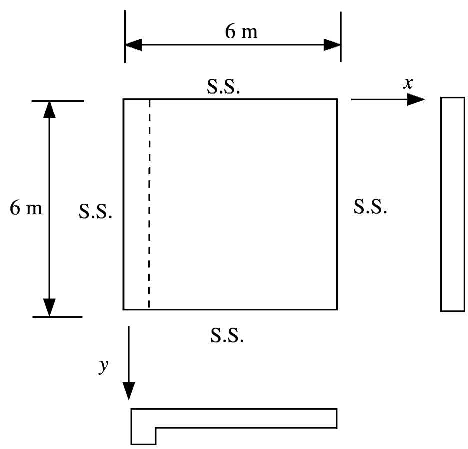

Figure 8. Plate with edge beam at $x = 0$, simply supported on four edges.

(simply supported edges) and a beam is present at only one edge. Equation (10) for such a plate can be written using only two sets of Ritz vectors,

$$w(x, y, t) = q_1(t)\phi_{pp}\phi_{pp} + q_2(t)\phi_{cp}\phi_{pp}. \tag{43}$$

If the geometrical and material properties for the plate and the beam shown in Figure 8 are identical to those shown in Figure 2 and described earlier, the fundamental plate frequency evaluated by using the above equation is found to be 10·3 Hz which is identical to that evaluated from a corresponding finite element analysis. The fundamental mode shape is compared in Figure 9.

Another situation, uncommon in civil structures but sometimes encountered in power plant and aerospace structural systems, is that of a beam with high torsional stiffness but low bending stiffness. For such an edge, the boundary condition can be represented as an intermediate between the pinned and the sliding (clamped edge on a roller) condition. For a plate shown in Figure 10, an edge beam is located at $x = 0$ and other three edges are simply supported. We can write

$$w(x, y, t) = q_1(t)\phi_{pp}\phi_{pp} + q_2(t)\phi_{sp}\phi_{pp}, \tag{44}$$

where the subscript *sp* represents a sliding condition at the plate edge with beam and a pinned condition at the other end. We encountered such a plate in a power plant structural system with $L_x, = 0{\cdot}84$ m, $L_y, = 1{\cdot}78$ m, $h_0 = 2{\cdot}667 \times 10^{-3}$ m, $E = 2{\cdot}0 \times 10^5$ Mpa, $v = 0{\cdot}3$

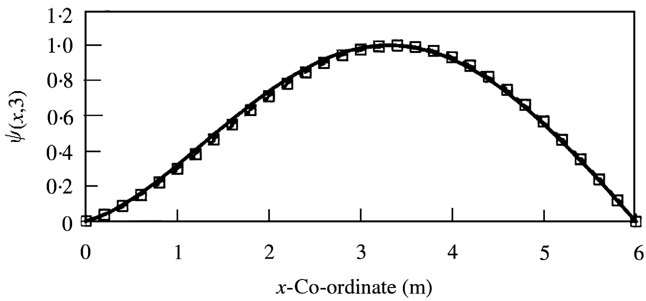

Figure 9. Fundamental mode shape at $y = 3\,\text{m}$, simply supported plate with edge beam at $x = 0$: —, finite element; - - □ - -, Ritz vector.

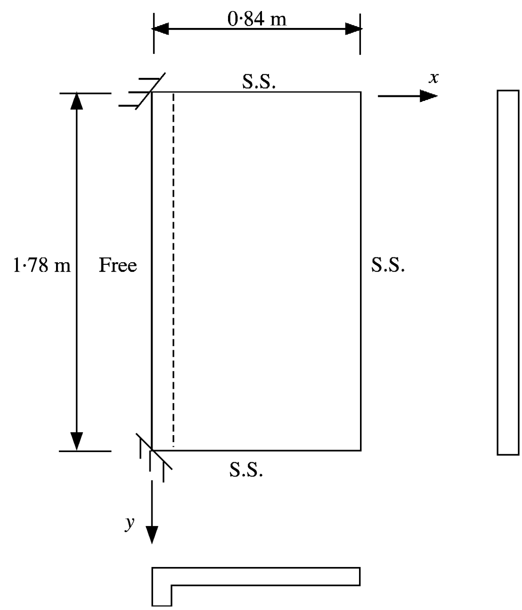

Figure 10. Plate with edge beam at $x = 0$, simply supported on three edges.

and $\rho = 31{\cdot}3\,\text{kg/m}^3$. The edge beam located at $x = 0$ had $I = 4{\cdot}0 \times 10^{-8}\,\text{m}^4$, $J = 4{\cdot}58 \times 10^{-10}\,\text{m}^4$ and $\mu = 0{\cdot}0139\,\text{kg/m}$. The fundamental frequency for this case calculated from the proposed approach was found to be 8·6 Hz. The corresponding value calculated from a finite element analysis is also 8·6 Hz. The mode shapes for this plate evaluated from the two analyses are compared in Figure 11.

Next, we illustrate the accuracy of the proposed approach for a series of solutions that are obtained by varying the bending and the torsional stiffness of edge beams in a plate shown in Figure 2. To start with, a high value is taken for the moment of inertia (high bending stiffness) of edge beams. Then, the torsional constant (torsional stiffness) of the edge beams is varied from a very low value (simply supported boundary condition) to a very high value (fixed boundary condition). Figure 12 compares the fundamental frequencies of the plate evaluated from the proposed approach with the corresponding values obtained from the finite element analyses.

To study this effect further, a very small value is taken for the torsional stiffness of the edge beams. Then, the moment of inertia is varied from a very low value (unrestrained

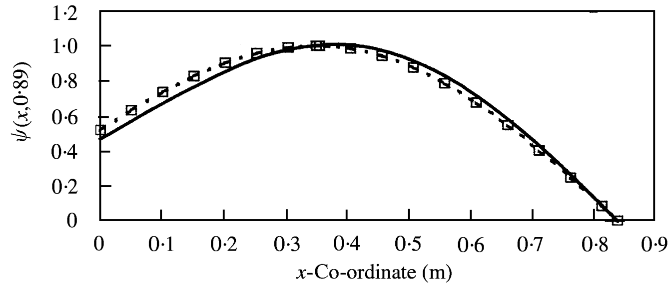

Figure 11. Fundamental mode shape at $y = 0{\cdot}89$ m, simply supported plate with beam at $x = 0$: —, finite element; - - □ - -, Ritz vector.

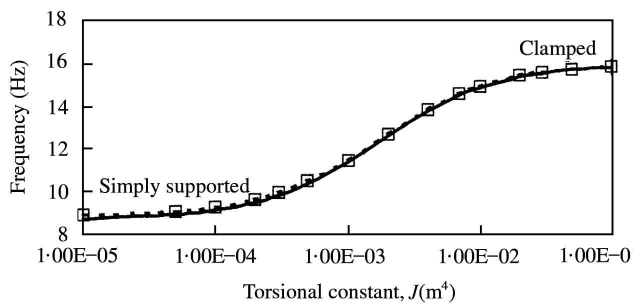

Figure 12. Variation of the fundamental frequency with the torsional stiffness of edge beams ($I = 0{\cdot}01$ m^4): —, finite element; - - □ - -, Ritz vector.

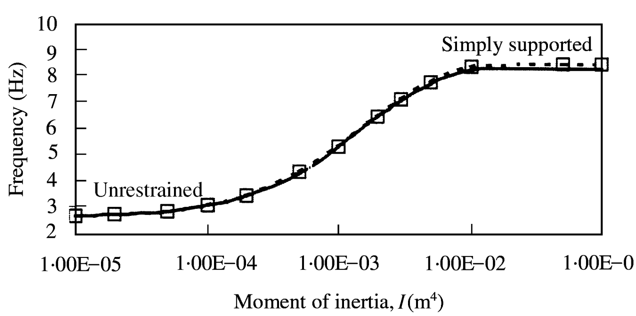

Figure 13. Variation of the fundamental frequency with the bending stiffness of edge beams ($J = 10^{-6}$ m^4): —, finite element; - - □ - -, Ritz vector.

boundary condition) to a very high value (simply supported boundary condition). Comparison of the fundamental frequencies for these cases with the corresponding finite element analyses results is shown in Figure 13.

6. STATIC ANALYSIS

The equivalent stiffness matrix, **K**, described earlier in equation (12) can also be used to perform a static analysis. The governing equation for a static load can be written as

$$\mathbf{K}\mathbf{q} = \mathbf{f}, \qquad (45)$$

in which **f** is the equivalent static load vector. For a uniformly distributed load $p(x, y)$ on the plate, the ith term in the equivalent load vector is given by

$$f_i = \int_0^{L_x} \int_0^{L_y} p\phi_{xi}(x)\phi_{yi}(y)\,\mathrm{d}x\,\mathrm{d}y. \tag{46}$$

For a concentrated load P at co-ordinate (x_0, y_0), the above expression becomes

$$f_i = P(x_0, y_0)\phi_{xi}(x_0)\phi_{yi}(y_0). \tag{47}$$

For uniformly distributed static loads, the proposed method gives accurate results by using the same Ritz vectors as those included in the evaluation of free vibration characteristics. For concentrated loads, the results obtained by using these vectors will be inaccurate. Consequently, one may use load-dependent Ritz vectors. This involves selection of mathematical functions that represent the static deformation shapes of a simple beam subjected to a unit load at the same location as that in the slab. As stated earlier, at least two Ritz vectors corresponding to two different idealized boundary conditions at the beam ends should be considered in order to account for an intermediate boundary condition. For example, consider a concentrated load of 100 kN at mid-span location of the plate shown in Figure 2. The corresponding static beam deformations, shown in Figure 14, for the clamped and pinned boundary conditions can be adopted as Ritz vectors, i.e.,

$$\phi_{pp} = \frac{x(3L^2 - 4x^2)}{L^3}, \qquad \phi_{cc} = \frac{4x^2(3L - 4x)}{L^3}, \quad 0 < x < \frac{L}{2}. \tag{48, 49}$$

The maximum plate deflection obtained by using the above equation in the proposed approach is 0·0075 m (0·75 cm) compared to 0·0078 m (0·78 cm) obtained from the corresponding finite element analysis. The displacement shapes at $y = 3$ m are compared in Figure 15. It should be noted that the self-weight of the plate and the beams was neglected

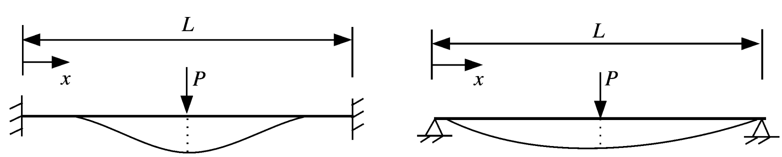

Figure 14. Displacement of beams subjected to concentrated load at mid-span: (a) clamped–clamped, $\Delta = (P/48EI)(3Lx^2 - x^3)$, $0 < x < L/2$; (b) pinned–pinned $\Delta = (P/16EI)(3L^2x - 4x^3)$, $0 < x < L/2$.

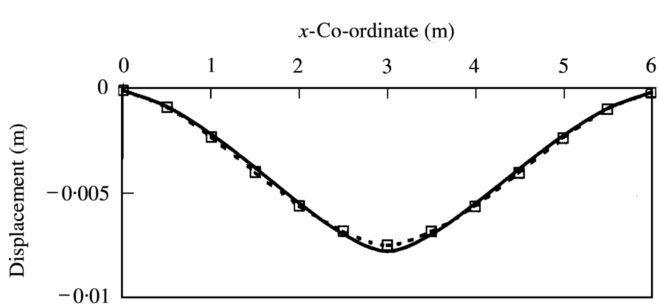

Figure 15. Displacement of the plate at $y = 3$ m, 100 kN concentrated load at mid-span location: —, finite element; - - □ - -, Ritz vector.

in the evaluation of the above results to study the accuracy of the proposed approach for concentrated static loads.

7. SUMMARY AND CONCLUSIONS

Several formulations have been presented over the years to evaluate the static and the dynamic characteristics of plates with elastic edge restraints. In most of the earlier studies, the bending and the torsional restraints are represented as stiffness coefficients with specified distributions along the plate edge. However, no formulations are presented to evaluate the distributions imparted by the presence of structural members such as beams along the plate edges. Recently, Takabatake and Nagareda [2] presented new formulations for evaluating the stiffness coefficients corresponding to edge beams which were then assumed to be uniformly distributed along the plate edges. In addition to the assumption of uniform distribution for the variation of stiffness coefficients along the plate edges, the effect of boundary conditions at the beam ends (plate corners) is included in terms of factors that are based on professional experience.

In this paper, a Ritz vector approach is developed based on the useful insights provided by Takabatake and Nagareda [2] as well as Warburton and Edney [8]. It avoids some of the assumptions made in these earlier studies and accounts for the actual bending and torsional characteristics of edge beams by including appropriate integrals in the Rayleigh–Ritz approach. Consequently, no assumption is needed to represent the effect of boundary conditions at the beam ends which is included in the proposed approach by considering the corresponding Ritz vectors. The proposed approach also accounts for the contribution of beam mass to the total kinetic energy, an effect that can be significant but is often neglected. Accuracy of the proposed approach is evaluated by comparison of the results with the corresponding values obtained from the finite element analyses. The results from the two sets of analyses for static loads as well as transverse plate vibrations in rectangular plates with different types of boundary conditions are found to be in good agreement with each other. It is shown that the evaluation of accurate results for concentrated static loads require consideration of load-dependent Ritz vectors in the proposed approach. For such loads, the Ritz vectors employed in the evaluation of transverse vibration characteristics would yield inaccurate results.

ACKNOWLEDGMENTS

This material is based upon work supported by the National Science Foundation under grant No. 0084551 and by the Center for Nuclear Power Plant Structures, Equipment and Piping at North Carolina State University. Resources for the Center come from the dues paid by member organizations and from the Civil Engineering Department and College of Engineering in the University.

REFERENCES

1. A. W. Leissa, P. A. A. Laura and R. H. Gutierrez 1979 *Journal of Acoustic Society of America* **66**, 180–184. Transverse vibrations of a circular plate having nonuniform edge constrains.
2. H. Takabatake and Y. Nagareda 1999 *Computers and Structures* **70**, 129–139. A simplified analysis of elastic plates with edge beams.

3. H. Takabatake 1991 *International Journal of Solids and Structures* **28**, 179–196. Static analyses of elastic plates with voids.
4. H. Takabatake 1991 *International Journal of Solids and Structures* **28**, 879–895. Dynamic analyses of elastic plates with voids.
5. H. Takabatake, H. Morimoto, T. Fujiwara and T. Honma 1996 *Computers and Structures* **58**, 263–275. Simplified analysis of circular plates including voids.
6. H. Takabatake, T. Imaizuni and K. Okatomi 1993 *Journal of Structural Engineering American Society of Civil Engineers* **121**, 28–38. Simplified analysis of rectangular plates with stepped thickness.
7. P. A. A. Laura and R. O. Grossi 1981 *Journal of Sound and Vibration* **75**, 101–107. Transverse vibration of rectangular plate elastically restrained against translation and rotation.
8. G. B. Warburton and S. L. Edney 1984 *Journal of Sound and Vibration* **95**, 537–552. Vibrations of rectangular plates with elastically restrained edges.
9. D. J. Gorman 1994 *Journal of Sound and Vibration* **174**, 451–459. A general solution for the free vibration of rectangular plates with arbitrarily distributed lateral and rotational elastic edge supports.
10. J. R. Vinson 1989 *The Behavior of Thin Walled Structures: Beams, Plates, and Shells*. Dordrecht: Kluwer.
11. R. Blevins 1979 *Formulas for Natural Frequency and Mode Shape*. New York: Van Nostrand Reinhold Company.
12. C. S. Kim, P. G. Young and S. M. Dickinson 1990 *Journal of Sound and Vibration* **143**, 379–394. On the flexural vibration of rectangular plates approached by using simple polynomials in the Rayleigh–Ritz method.
13. Z. Ding 1995 *Computers and Structures* **57**, 731–735. Natural frequencies of elastically restrained rectangular plates using a set of static beam functions in the Rayleigh–Ritz method.
14. G. N. Geannakakes 1995 *Journal of Sound and Vibration* **182**, 141–478. Natural frequencies of arbitrarily shaped plates using the Rayleigh–Ritz method together with natural co-ordinate regions and normalized characteristic orthogonal polynomials.
15. C. Rajalingham, R. B. Bhat and G. D. Xistris 1996 *Journal of Sound and Vibration* **193**, 497–509. Vibration of rectangular plates using plate characteristic functions as shape functions in the Rayleigh–Ritz method.